Reaction Pathway and Rate-Determining Step in the Aminoacylation of $tRNA^{Arg}$ Catalyzed by the Arginyl-tRNA Synthetase from Yeast†

Alan R. Fersht,* Jean Gangloff, and Guy Dirheimer

ABSTRACT: The arginyl-tRNA synthetase from yeast, which does not form an isolable aminoacyl adenylate complex or catalyze the pyrophosphate-exchange reaction in the absence of tRNA, is one of the strongest candidates for the concerted mechanism. This pathway is shown not to occur by measurements of the rate of the reverse reaction, the AMP/PP_i dependent deacylation of Arg-$tRNA^{Arg}$. The reversal of the overall aminoacylation reaction, measured under single-turnover conditions of excess enzyme over tRNA, is too slow to account for the *initial* rate of the pyrophosphate-exchange reaction. Further, direct evidence is presented that the reverse reaction takes place in two chemical steps: on mixing the enzyme with Arg-$tRNA^{Arg}$ and AMP there is a partial deacylation of the aminoacyl-tRNA which occurs with the same initial rate as when PP_i is present. Combined with the circumstantial evidence from other workers that the enzyme can utilize exogenous arginyl adenylate, this is good evidence that the AMP/PP_i dependent deacylation of Arg-tRNA takes place in a stepwise reaction, i.e., slow formation of E·Arg–AMP followed by rapid pyrophosphorolysis. Hence, from the principle of microscopic reversibility, the aminoacylation reaction is also stepwise, with pyrophosphate exchange in the initial stages of aminoacylation taking place by the reversal of the formation of arginyl adenylate. Rapid quenching and sampling experiments on the millisecond scale of the aminoacylation reaction at pH 7.2 and below show that there is rapid formation of nearly 1 mol of Arg-tRNA per mol of enzyme prior to the steady-state turnover. The rate-determining step in aminoacylation is the release of Arg-tRNA from the enzyme. At higher pH, the burst decreases as release becomes more rapid. Closer examination of the pre-steady-state phase reveals a lag period prior to the exponential. This is characteristic of a three (or higher) step reaction, as expected for the sequence: formation of Arg-AMP, transfer of Arg to tRNA, release of Arg-tRNA. The solution of the rate equations for this scheme is given, and the individual rate constants for activation, transfer, and release are tentatively derived from the data at pH 7.2 in combination with additional experimental evidence.

The old adage that "kinetics can never prove mechanisms but only eliminate alternative pathways" applies only to steady-state kinetics where intermediates are not directly observed. When the rates of formation and decay of reaction intermediates are directly monitored, a particular reaction pathway may be established or "proved" with the same degree of rigor as for most chemical and biochemical experiments, *provided* the following three criteria are obeyed: the intermediate is isolated and characterized; it is formed fast enough to be on the reaction pathway; it reacts fast enough to be on the reaction pathway (cf. Jencks, 1969). Using these criteria, we have established the aminoacyl adenylate pathway for representative members of all the structural classes of aminoacyl-tRNA synthetases that form an isolable aminoacyl adenylate complex in the absence of tRNA (isoleucyl-, tyrosyl-, phenylalanyl-, methionyl, valyl- and cysteinyl-tRNA synthetases; Fersht and Kaethner, 1976; Fasiolo and Fersht, 1978; Mulvey and Fersht, manuscript in preparation; Mulvey et al., manuscript in preparation (1978). However, this rigorous kinetic approach could not be applied to the arginyl-, glutamyl- and glutaminyl-tRNA synthetases because they do not form an isolable aminoacyl adenylate complex in the absence of tRNA (Mehler and Mitra, 1967; Ravel et al., 1965).

These latter enzymes do not catalyze the pyrophosphate-exchange reaction in the absence of tRNA. This has led to the suggestion that the aminoacylation reaction does not proceed by the aminoacyl adenylate route (eq 1) but by a concerted pathway (eq 2; Loftfield, 1972).

$$\text{E·AA·ATP·tRNA} \rightleftharpoons \text{E·AA-AMP·tRNA} + PP_i \rightleftharpoons \text{E} + \text{AA-tRNA} + \text{AMP} + PP_i \quad (1)$$

$$\text{E·AA·ATP·tRNA} \rightleftharpoons \text{E·AA-tRNA·AMP·}PP_i \rightleftharpoons \text{E} + \text{AA-tRNA} + \text{AMP} + PP_i \quad (2)$$

In support of the aminoacyl adenylate pathway for the arginyl-tRNA synthetase, Mehler and Mitra (1967) and Nazario and Evans (1972) have shown that the enzymes from *Escherichia coli* and *Neurospora* can utilize exogenous, chemically synthesized, arginyl adenylate in the pyrophosphorolysis and aminoacylation reactions. However, there is no direct evidence that the adenylate is formed on the reaction pathway (Craine and Peterkofsky, 1975).

In the present study, we first establish the rate-determining step of the aminoacylation reaction catalyzed by the arginyl-tRNA synthetase from yeast using quenched-flow methods. Then, by measuring the rate of the reverse reaction, the AMP/PP_i dependent deacylation of Arg-tRNA, we show that the pyrophosphate-exchange reaction is too fast to be accounted for by the reverse of the simple concerted mechanism of eq 2. The reverse reaction is shown to proceed in a stepwise manner, consistent with the reversal of eq 1.

Experimental Procedures

Apparatus. The quenched-flow and pulsed-quenched-flow apparatus described by Fersht and Jakes (1975) was used for the rapid-quenching and sampling experiments, except for the following modification. Previously, in the pulsed mode, the reagents were flushed out of the incubation tube by a pulse of

† From the MRC Laboratory of Molecular Biology, Cambridge CB2 2QH, England (A.R.F.) and the Laboratoire de Biochimie, Institut de Biologie Moleculaire et Cellulaire du Centre National de la Recherche Scientifique, Strasbourg, France. *Received February 2, 1978.*

0006-2960/78/0417-3740$01.00/0

distilled water entering immediately above the first mixing chamber so that a small amount of "unincubated" material was expelled with the incubated mix. This is now avoided by the flushing solution entering immediately below the mixing chamber.

Materials. The arginyl-tRNA synthetase from yeast (*Saccharomyces cerevisiae,* strain 836) was prepared as described previously (Gangloff et al., 1976). $tRNA^{Arg}_{III}$ (arginine acceptance = 1.7 nmol/A_{260} unit) was the generous gift of J. Weissenbach. [^{14}C]Arg-tRNA was prepared by incubating $tRNA^{Arg}_{III}$ (0.3 mg) in a solution (0.33 mL) containing arginyl-tRNA synthetase (2 μM), ATP (3 mM), [^{14}C]Arg (70 μM, 324 mCi/mmol), inorganic pyrophosphatase (0.5 unit), $MgCl_2$ (10 mM), and Tris-Cl[1] (44 mM, pH 7.78). After 2 min, the solution was extracted with phenol [0.35 mL of saturated solution plus 0.02 mL of sodium acetate buffer (2 M, pH 5)]. The charged tRNA was precipitated from the aqueous layer by the addition of 2 volumes of ethanol. After gel filtration (Sephadex G-25, 10 mM $MgCl_2$), a near quantitative yield of [^{14}C]Arg-tRNA charged to 1.7 nmol/A_{260} was obtained.

Kinetic Procedures

The following buffers were used: 14 mM Bistris-Cl, pH 5.4–6.0; 50 mM Tris-Cl, pH 7.2; 144 mM Tris-Cl, pH 7.78 (all containing 10 mM $MgCl_2$, 0.1 mM phenylmethanesulfonyl fluoride, and 10 mM mercaptoethanol). All experiments were performed at 25 °C, unless otherwise stated.

Determination of Enzyme Concentration. Protein concentrations were determined from the absorbance (A_{280} = 1.26 mg mL^{-1} cm^{-1}) using a molecular weight of 73 000. The number of binding sites for arginine was determined by equilibrium dialysis. One-half of each cell contained enzyme (4.35 μM) and $tRNA^{Arg}_{III}$ (10 μM) in Tris-Cl (50 mM, pH 7.8), mercaptoethanol (1 mM), and glycerol (15%). The other half contained various concentrations of [^{14}C]Arg (148 mCi/mmol, 3–60 μM) in the same buffer. Samples were assayed after 5 h of equilibration at 4 °C. The stoichiometry of binding of tRNA was measured by the nitrocellulose filter assay of Yarus and Berg (1970). The efficiency of the binding of the E·[^{14}C]Arg-$tRNA^{Arg}$ to the filter was first checked by measuring the amount of radioactivity bound on passing a mixture of charged tRNA with an excess of enzyme at a concentration of greater than 100 times the dissociation constant. Samples (100 μL) containing enzyme (28 μM), [^{14}C]Arg-$tRNA^{Arg}$ (0.16–0.18 μM), bovine serum albumin (10 mg/L), $MgCl_2$ (10 mM), and phosphate buffer (10 mM, pH 6.0) were filtered on nitrocellulose disks (Sartorius 0.45 μm) and washed twice with 2-mL portions of the same buffer. The binding curve for Arg-tRNA was constructed in a like manner, except that the concentration of enzyme was 2.8 μM and that of [^{14}C]Arg-$tRNA^{Arg}$ varied from 0.2 to 6 μM. The data were corrected for the value of 71% efficiency of binding measured above.

Pyrophosphate-Exchange Kinetics. The initial rate of exchange of ^{32}P-labeled pyrophosphate (1 or 2 mM) into ATP (10 mM) in the presence of arginine (20 mM) and tRNA catalyzed by the enzyme was measured at various values of pH by the conventional procedure of quenching aliquots of the reaction mixture with a suspension of charcoal (1%) in perchloric acid (3.5%), collecting the precipitate on a Whatman GF/C filter, and monitoring the adsorbed [^{32}P]ATP using a gas-flow counter.

[1] Abbreviations used are: Tris-Cl, 2-amino-2-hydroxymethyl-1,3-propanediol chloride; Bistris-Cl, 2-[bis(2-hydroxyethyl)amino]-2-(hydroxymethyl)-1,3-propanediol chloride; Hepes, 4-(2-hydroxyethyl)-1-piperazineethanesulfonic acid.

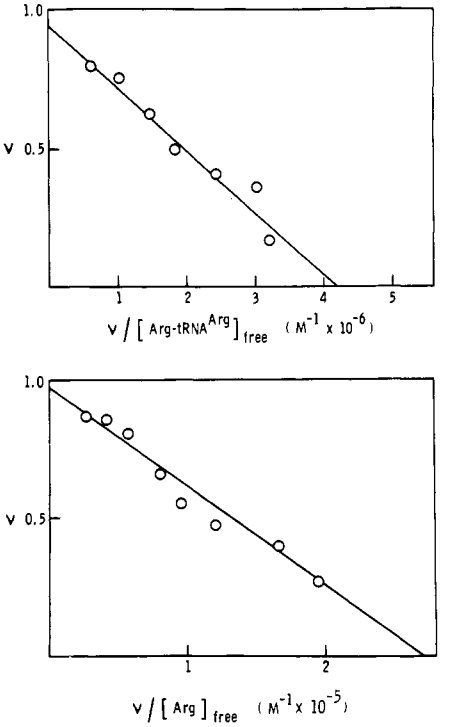

FIGURE 1: Determination of stoichiometry of binding of arginine and $tRNA^{Arg}$ (see text).

The Extent of Charging under Pyrophosphate Exchange Conditions. Aliquots of a solution containing [^{14}C]Arg (20 μM), ATP (10 mM), tRNA (4 μM), enzyme (67 nm), and inorganic pyrophosphatase (5 units/mL) in the standard pH 7.78 buffer were quenched with trichloroacetic acid (5%). The precipitates were collected on Millipore filters, and, after washing and drying, the radioactivity was measured by scintillation counting using a toluene-based scintillant. The procedure was repeated substituting pyrophosphate (1 mM) for the inorganic pyrophosphatase.

Initial Rate of Aminoacylation of tRNA. One syringe of the quenched-flow or pulsed-quenched-flow apparatus contained enzyme (256 nM) and tRNA (4.0 μM) in the appropriate standard buffer solution, while the other contained [^{14}C]Arg (40 μM), ATP (20 mM), and inorganic pyrophosphatase. Equal volumes were mixed and quenched with trichloroacetic acid, and the precipitates were collected and assayed as above.

AMP/PP_i Dependent Enzyme-Catalyzed Deacylation of Arg-tRNA. The rate constant for the reverse reaction was measured under pseudo-first-order conditions. Enzyme (0.71 μM) was added to [^{14}C]Arg-tRNA (0.068 μM), pyrophosphate (2 mM), and various concentrations of AMP in the standard buffers (containing 2 rather than 10 mM $MgCl_2$). Aliquots were added to trichloroacetic acid and the precipitates assayed for radioactivity as above.

Results

Concentration of Active Enzyme. The methods of active-site titration we have used previously to measure the concentration of active enzyme (Fersht et al., 1975) are not applicable to the arginyl-tRNA synthetase, since it does not form an aminoacyl adenylate complex in the absence of tRNA. The concentration was thus determined from the number of amino acid binding sites found from equilibrium dialysis experiments, a procedure found to agree well with active-site titration (Mulvey and Fersht, 1977). In the presence of tRNA (Figure 1), the enzyme

TABLE I: Pyrophosphate-Exchange Kinetics.[a]

pH	enzyme (nM)	PP_i (mM)	k^b (s^{-1})
5.35	128	2	0.8
6.0	128	2	8.4
	128	1	7.1
7.20[c]	11	2	47
		1	47
7.78[d]	6	2	

[a] 25 °C, 10 mM ATP, 10 mM $MgCl_2$, 2 μM tRNA. [b] $k = V_0/[E]$. [c] 12 μM tRNA. [d] Charging of tRNA completed before appreciable pyrophosphate exchange.

TABLE II: Extent of Charging of tRNA under Pyrophosphate Exchange and Aminoacylation Conditions.[a]

time (s)	[Arg-tRNA] (μM) aminoacylation (+ PPase)	[Arg-tRNA] (μM) PP exchange (+ 1 mM PP_i)
0	0	0
45	4.01	3.46
90	3.99	3.79
150	3.97	3.79

[a] 25 °C, 10 mM $MgCl_2$, pH 7.78, 4 μM tRNA, 67 nM enzyme, 10 mM ATP, and 20 μM [^{14}C] Arg.

TABLE III: Initial Rate of Charging of tRNA.[a]

pH	exponential phase k (s^{-1})[b]	exponential phase amplitude[c]	steady state k (s^{-1})[d]
5.8	1.3	0.6 ± 0.01	0.04 ± 0.001
6.0	1.7	0.66 ± 0.02	0.090 ± 0.003
7.20	33	0.68 ± 0.03	2.78 ± 0.06
7.78		0.4 ± 0.1	9.0 ± 1

[a] 25 °C, 10 mM $MgCl_2$, 20 μM [^{14}C]Arg, 10 mM ATP, 2 μM tRNA, and 128 nM enzyme. [b] Exponential part of trace. [c] Moles of Arg-tRNA per mole of enzyme. [d] Turnover of moles of Arg-tRNA per mole of enzyme per second.

binds 0.97 mol of arginine per polypeptide chain of molecular weight 73 000. The dissociation constant of arginine at 4 °C, pH 7.8 (50 mM Tris-Cl, 1 mM mercaptoethanol), and 15% glycerol is 4.0 μM. The stoichiometry of tRNA binding was determined by the nitrocellulose filtration procedure as a further check and found to be 0.94 with a dissociation constant of 0.22 μM.

Pyrophosphate-Exchange Kinetics. The values of k in Table I are close to the turnover numbers, since the reagent concentrations are all about 6 to 20 times higher than the values of K_M (Gangloff et al., 1976). The turnover number decreases with decreasing pH below pH 7.2. However, it was found that the exchange rate at pH 7.78 appears to be very slow. The reason for this is due to an experimental artifact. Under the reaction conditions, nearly all the tRNA is rapidly aminoacylated before significant exchange occurs. It is seen in Table II that by using 67 nM enzyme 95% of the tRNA is aminoacylated after 90 s at pyrophosphate-exchange conditions (cf. Papas and Peterkofsky, 1972). Thus, an equilibrium is reached in which most of the tRNA is aminoacylated, and the exchange of pyrophosphate into ATP is slow because either the reverse reaction is slow or abortive complexes accumulate. This problem arises at higher pH, since, as seen below, the charging rate increases rapidly with pH.

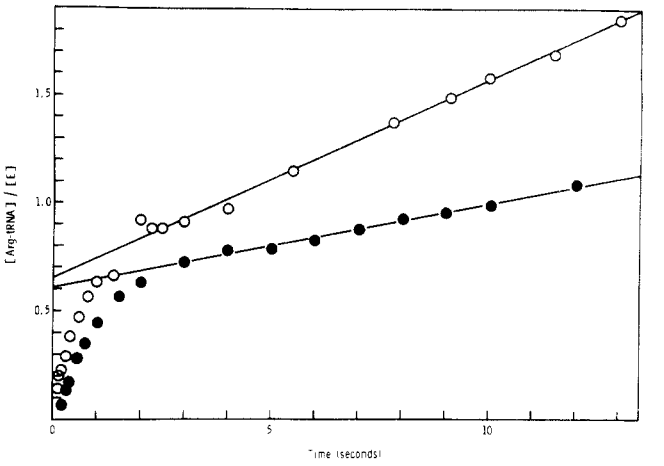

FIGURE 2: The initial rate of formation of Arg-tRNA^{Arg} at pH 5.8 (●) and 6.0 (○). (Conditions are given in Table III.)

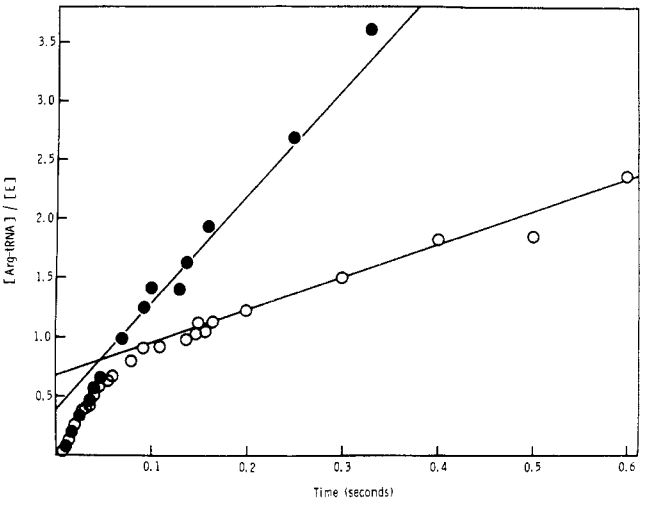

FIGURE 3: The initial rate of formation of Arg-tRNA^{Arg} at pH 7.2 (○) and pH 7.78 (●). (Conditions are given in Table III.)

Aminoacylation Kinetics. The initial rate of charging of tRNA is different kinetically from all the other aminoacyl-tRNA synthetases investigated in this laboratory. In all other cases the initial rate of charging is a simple linear curve which extrapolates back through the origin of the graph. However, it is seen in Figures 2 and 3 that "burst" kinetics hold. There is an initial exponential phase followed by a steady-state turnover of substrate. At pH 5.8 to 7.2, the steady-state portion of the curve extrapolates back to a "burst" of 0.6 to 0.7 mol of tRNA charged per mol of enzyme. At pH 7.78, the burst drops to about 0.4 (Figure 3). The data are listed in Table III.

The occurrence of a burst of formation of aminoacyl-tRNA followed by a steady-state turnover is precisely the behavior predicted for the rate-determining step (at saturating reagent concentrations) being the release of the charged tRNA from the enzyme (Fersht and Jakes, 1975).

A closer examination of the pre-steady-state phase of the charging reveals that it is *biphasic* (Figure 4). There is a distinct lag in the production of Arg-tRNA with time (Figure 4, inset). This is apparent as an initial curvature in the semilogarithmic plot. The rate constant for the exponential increase after the lag in each case is listed in Table III. The detailed analysis of such curves is given in the Appendix. Nevertheless, it can be said immediately that the lag indicates that there is at least one kinetically important intermediate on the reaction pathway.

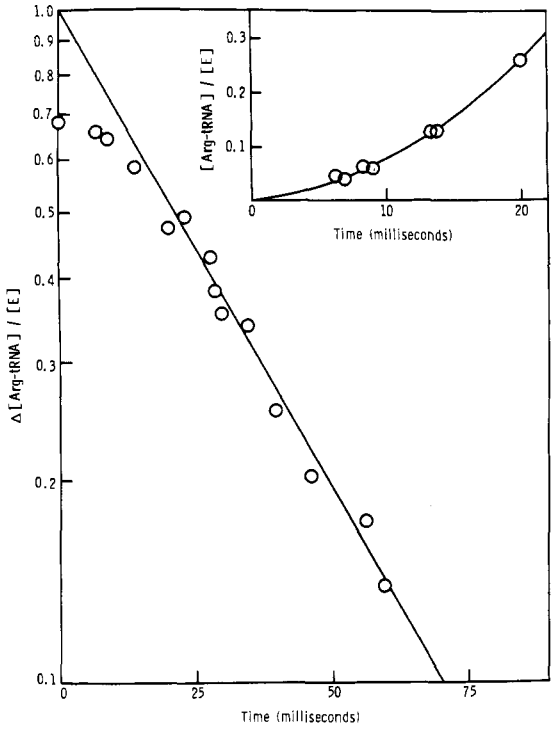

FIGURE 4: Semilogarithmic plot of the pre-steady-state phase of aminoacylation at pH 7.2; see Appendix, eq 22A. *Inset:* The "lag period" preceding the exponential phase—the solid curve is calculated from eq 12A of the Appendix using the derived values of k_1, k_2, and k_3 assuming the simple three-step reaction of eq 1a of the Appendix.

The Reverse Reaction—The AMP/PP$_i$ Dependent Deacylation of Arg-tRNA. The reaction was studied under single-turnover conditions. That is, the rate of deacylation of Arg-tRNA was measured in the presence of PP$_i$ and AMP and an *excess* of enzyme over total tRNA and Arg-tRNA. The reaction was followed in this way rather than by the usual technique of excess tRNA over enzyme to ensure that the rate measured is that of the deacylation step rather than the slow dissociation of tRNA from the E·ATP·AA·tRNA complex. This is a necessary and real precaution, since it was seen above for the forward aminoacylation reaction that the first 0.6 to 0.7 mol of Arg-tRNA is formed rapidly, while the rate-limiting step for further reaction is the dissociation of the Arg-tRNA from the enzyme. Complications caused by product inhibition by tRNA are also avoided with the single-turnover method. It is seen in Figure 5 that the deacylation reaction follows good first-order kinetics. The rate constant for this reaction is about 0.07 s^{-1} and pH 6.0. This is some two orders of magnitude slower than the turnover number for pyrophosphate exchange under similar conditions (Table I).

The reaction was studied at pH 6.0 because it is sufficiently slow to be followed by hand. The deacylation reaction is also too slow at higher values of pH to account for pyrophosphate exchange. For example, at pH 7.2 and 20 μM AMP (a concentration below the K_M but still vastly above the [AMP] accumulating in the initial rate reactions) the observed deacylation rate constant is only 0.1 s^{-1}, compared with a turnover number of 47 s^{-1} for exchange (Table I).

Two control experiments were performed to check that the single turnover experiments are not artifactual. In one experiment in Table IV, equimolar concentrations of enzyme and Arg-tRNA (0.72 μM) were used. Under these conditions, the kinetics are no longer first order. However, the initial rate of reaction indicated a rate constant of about 0.08 s^{-1} at pH 6.0, a value close to the other experiments. This was then repeated,

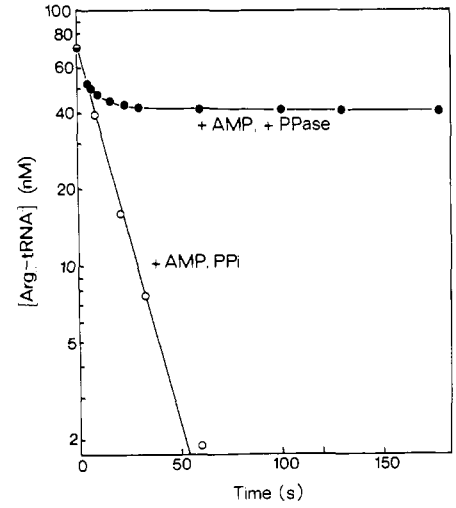

FIGURE 5: The AMP/PP$_i$ dependent deacylation of Arg-tRNA at pH 6 (conditions as in Table IV, 0.72 μM enzyme and 0.07 μM [^{14}C]Arg-tRNA): (○) 2 mM AMP and 2 mM PP$_i$; (●) 2 mM AMP and no PP$_i$ (plus inorganic pyrophosphatase).

TABLE IV: AMP/PP$_i$ Dependent Deacylation of Arg-tRNA^{Arg}.[a]

pH	enzyme (μM)	Arg-tRNA (μM)	AMP (mM)	k^b (s^{-1})
6.0	0.72	0.07	0	stable
6.0	0.36	0.07	0.5	0.069
6.0	0.72	0.07	0.5	0.074
6.0	0.72	0.07	2.0	0.069
6.0	0.72	0.72	2.0	~0.08[c]
7.20	0.72	0.07	0.02	0.10
7.20	0.72	0.07	2.0	>0.3[d]

[a] 25 °C, 2 mM PP$_i$, 2 mM $MgCl_2$. [b] First-order rate constant measured under pseudo-first-order conditions of [E] ≫ [Arg-tRNA]. [c] Initial slope as second order conditions. [d] Too fast to be measured manually.

lowering the enzyme concentration to 80 nm. The concentration of Arg-tRNA decreased with about the same initial rate as before, but the reaction rate slowed down considerably after the first turnover, vindicating the decision to follow the reaction under single-turnover conditions.

Partial Reversal of Aminoacylation in the Absence of Pyrophosphate. It is seen in Figure 5 (●) that there is partial deacylation of the Arg-tRNA when it is mixed with excess enzyme in the presence of AMP but in the absence of PP$_i$. Furthermore, the initial rate of reaction is the same as when the reaction mixture included PP$_i$. The partial reversal is attributed to the formation of some enzyme-bound Arg-AMP and tRNA followed by dissociation and partition of the products to displace the equilibrium (eq 3). The decrease in

$$\text{E·AMP·AA-tRNA} \rightleftharpoons \text{E·AA-AMP·tRNA} \rightleftharpoons \text{E·tRNA} + \text{E·AA-AMP} + \text{tRNA} + \text{AA-AMP} \quad (3)$$

concentration of Arg-tRNA is about 43% and takes place with a first-order rate constant of about 0.18 s^{-1}. That this is a reversible reaction is shown by the experiment in Figure 6. On addition of 2 mM AMP to a reaction mixture containing 2 μM enzyme and 1 μM Arg-tRNA at 0 °C, pH 7.5 (50 mM Hepes and 10 mM $MgCl_2$), there is an initial drop of about 30% of the Arg-tRNA. But on increasing the tRNA to 20 μM, the level of charging is partially restored. The partial deacylation is not caused by residual PP$_i$ in the solutions, since incubation of the reaction mixture and enzyme solution with inorganic

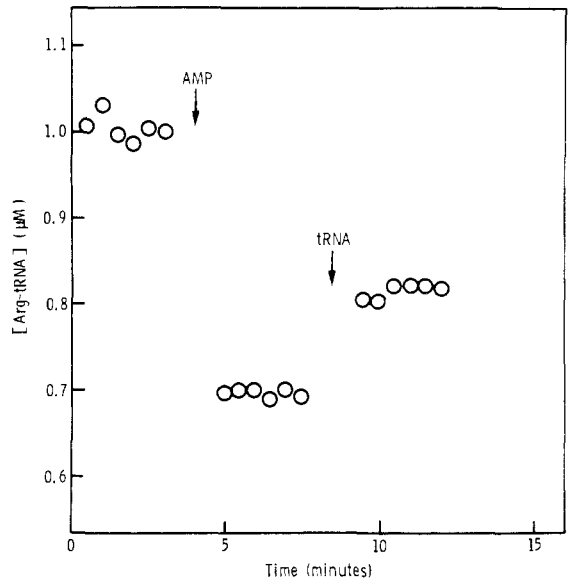

FIGURE 6: The Arg-tRNA + AMP ⇌ Arg-AMP + tRNA reaction. AMP (2 mM) is added to a solution of Arg-tRNA (1 μM) and arginyl-tRNA synthetase at pH 7.5 and 0 °C where indicated. Additional tRNA (20 μM) is then added where indicated (see text).

pyrophosphatase prior to mixing does not affect the rate or size of the change.

Discussion

Establishing the Stepwise Mechanism. The arginyl-tRNA synthetase from yeast catalyzes the exchange of pyrophosphate into ATP in the presence of arginine and tRNA at pH values lower than 7.2 far more rapidly than the steady-state formation of Arg-tRNA in the absence of pyrophosphate (Tables I and III). The low steady-state rate of charging is caused by the fact that the release of the Arg-tRNA from the enzyme is slow and rate determining. The first mole of charged tRNA is formed rapidly with complex biphasic kinetics (see Appendix), the rate constants of which are of the same order of magnitude as those for the pyrophosphate-exchange reaction (Figures 2–4).

The proposed "concerted" mechanism in which the ternary complex E·ATP·Arg·tRNA forms E·AMP·PP_i·Arg-tRNA without an aminoacyl adenylate or any other chemically activated intermediate may be ruled out by a comparison of the pyrophosphate-exchange reaction and the reverse reaction, the AMP/PP_i dependent deacylation of Arg-tRNA. The aminoacyl adenylate and concerted mechanisms predict different pathways for the exchange of pyrophosphate into ATP. In the aminoacyl adenylate, route exchange occurs before the tRNA is charged (eq 4) while the concerted mechanism requires exchange by the reversal of the charging reaction (eq 5).

$$\text{E·ATP·Arg·tRNA} \rightleftharpoons \text{E·PP}_i\text{·Arg-AMP·tRNA} \quad (4)$$

$$\text{E·ATP·Arg·tRNA} \rightleftharpoons \text{E·PP}_i\text{·AMP·Arg-tRNA} \quad (5)$$

We have measured the rate of the reversal of charging (Table IV) and found it to be at least 100 times slower than exchange at pH 6.0 and 7.2. This would appear to eliminate the concerted mechanism, but, as in most reaction schemes where the intermediate states are not observed directly, it can be resurrected by assuming that there is an additional intermediate on the reaction pathway—not a chemical intermediate but a different conformational state of the enzyme involving a slow conformational change (eq 6). This allows a rapid exchange of pyrophosphate at the first fast step. The overall rate of charging and the rate of overall reversal are limited by the

$$\text{E·ATP·Arg·tRNA} \overset{\text{fast}}{\rightleftharpoons} \text{E*·PP}_i\text{·AMP·Arg-tRNA} \overset{\text{slow}}{\rightleftharpoons} \text{E·PP}_i\text{·AMP·Arg-tRNA} \overset{\text{fast}}{\rightleftharpoons} \text{E} + \text{PP}_i + \text{AMP} + \text{Arg-tRNA} \quad (6)$$

rate of the slow conformational change between E* and E at the second step. The observed "burst" kinetics of aminoacylation are also consistent with this scheme—the release of Arg-tRNA from the enzyme is slow because it is limited by the slow conformational change.

A second, but highly unlikely, kinetic situation that could account for the rapid pyrophosphate exchange on the concerted scheme is that the exchange is a parallel side reaction that is dependent on both $tRNA^{Arg}$ and arginine and is inhibited by Arg-$tRNA^{Arg}$.

However, there is direct evidence that the reversal takes place in two *chemical* steps. As seen in Figure 5 (●), when the enzyme is added to a solution containing Arg-tRNA and AMP but no PP_i, deacylation occurs with the same initial rate as when PP_i is present but then slows down when an equilibrium is reached (pyrophosphate is required to push the reaction to completion). Deacylation thus proceeds by eq 7.

$$\text{E·AMP·Arg-tRNA} \overset{\text{slow}}{\rightleftharpoons} \text{E·AMP-Arg·tRNA} \overset{\text{fast}}{\underset{\text{PP}_i}{\rightleftharpoons}} \text{E·ATP·Arg·tRNA} \quad (7)$$

The case for the intermediate in equation 7 being the aminoacyl adenylate is based on the argument of Jencks (1969) termed *generalization:* this intermediate has been established for other aminoacyl-tRNA synthetases and all evidence is consistent with this. Further, it has been shown that the enzyme can utilize chemically synthesized arginyl adenylate in the presence of tRNA (Mehler and Mitra, 1967; Nazario and Evans, 1974). It is also very difficult to suggest an alternative chemically reasonable mechanism for the AMP-stimulated deacylation of Arg-tRNA.

Nature of the Rate-Determining Step in Aminoacylation. The "burst" kinetics indicate that the release of Arg-tRNA is slow and rate determining at saturating concentrations of substrates. This could be due to either the slow dissociation of an E·Arg-tRNA complex or, as suggested for eq 6, the release of Arg-tRNA being limited by a slow conformational change. The rate-determining release of NADH from some dehydrogenases is accompanied by a conformational change. In these situations it is difficult to resolve whether the conformational change precedes or is concurrent with dissociation.

Appendix

Transient State Rate Equations for Reaction Involving Two Intermediates:

$$\underset{(A)}{\text{E·tRNA·AA·ATP}} \xrightarrow{k_1} \underset{(B)}{\text{E·AA-AMP·tRNA}} \xrightarrow{k_2} \underset{(C)}{\text{E·AA-tRNA}} \xrightarrow{k_3} \text{E} + \text{AA-tRNA} \quad (1A)$$

In eq 1A where tRNA, AA, and ATP are at saturating concentrations, the concentrations of A, B, and C in the steady state are given by:

$$[A_{SS}] = k_2k_3[A_0]/(k_1k_2 + k_2k_3 + k_3k_1) \quad (2A)$$

$$[B_{SS}] = k_1k_3[A_0]/(k_1k_2 + k_2k_3 + k_3k_1) \quad (3A)$$

$$[C_{SS}] = k_1k_2[A_0]/(k_1k_2 + k_2k_3 + k_3k_1) \quad (4A)$$

At the initial stages of the reaction and when tRNA, AA, and ATP bind rapidly to the enzyme, eq 1A reduces to reaction 5A.

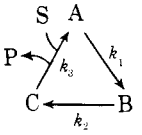

(5A)

The pre-steady-state rate equations may then be solved by the usual procedures (Frost and Pearson, 1961) using the boundary conditions of eq 2A, 3A, and 4A and also at $t = 0$, $[A] = [A_0]$, and $[B_0] = [C_0] = 0$, to give:

$$[A] = [A_0]\left\{\frac{k_2k_3}{\lambda_2\lambda_3} + \frac{1}{(\lambda_2-\lambda_3)}\left[k_1 - \lambda_3 + \frac{k_2k_3}{\lambda_2}\right]e^{-\lambda_2 t} + \frac{1}{(\lambda_3-\lambda_2)}\left[k_1 - \lambda_2 + \frac{k_2k_3}{\lambda_3}\right]e^{-\lambda_3 t}\right\} \quad (6A)$$

$$[B] = [A_0]\left\{\frac{k_1k_3}{\lambda_2\lambda_3} + \frac{k_1}{(k_2-\lambda_2)(\lambda_2-\lambda_3)}\left[k_1 - \lambda_3 + \frac{k_2k_3}{\lambda_2}\right]e^{-\lambda_2 t} + \frac{k_1}{(k_2-\lambda_3)(\lambda_3-\lambda_2)}\left[k_1 - \lambda_2 + \frac{k_2k_3}{\lambda_3}\right]e^{-\lambda_3 t}\right\} \quad (7A)$$

$$[C] = [A_0]\left\{\frac{k_1k_2}{\lambda_2\lambda_3} + \frac{k_1-\lambda_2}{k_3(\lambda_2-\lambda_3)}\left[k_1 - \lambda_3 + \frac{k_2k_3}{\lambda_2}\right]e^{-\lambda_2 t} + \frac{k_1-\lambda_3}{k_3(\lambda_3-\lambda_2)}\left[k_1 - \lambda_2 + \frac{k_2k_3}{\lambda_3}\right]e^{-\lambda_3 t}\right\} \quad (8A)$$

where:

$$\lambda_2,\lambda_3 = \frac{[k_1 + k_2 + k_3 \pm \sqrt{(k_1 + k_2 + k_3)^2 - 4(k_1k_2 + k_2k_3 + k_1k_3)}]}{2} \quad (9A)$$

The manipulations are simplified by the relationships:

$$\lambda_2 + \lambda_3 = k_1 + k_2 + k_3 \quad (10A)$$

and

$$\lambda_2\lambda_3 = k_1k_2 + k_2k_3 + k_3k_1 \quad (11A)$$

The concentration of AA-tRNA, including that bound to the enzyme, is given by:

$$[\text{AA-tRNA}] = [A_0]\left\{\frac{k_1k_2}{\lambda_2\lambda_3}\left[1 - \frac{k_3(\lambda_2+\lambda_3)}{\lambda_2\lambda_3}\right] + \frac{k_1k_2k_3t}{\lambda_2\lambda_3} + \frac{(\lambda_2-k_3)(k_1-\lambda_2)}{\lambda_2k_3(\lambda_2-\lambda_3)}\left[k_1 - \lambda_3 + \frac{k_2k_3}{\lambda_2}\right]e^{-\lambda_2 t} + \frac{(\lambda_3-k_3)(k_1-\lambda_3)}{\lambda_3k_3(\lambda_3-\lambda_2)}\left[k_1 - \lambda_2 + \frac{k_2k_3}{\lambda_3}\right]e^{-\lambda_3 t}\right\} \quad (12A)$$

After sufficient time for the exponential terms to die out ($t > 10/\lambda_2$ or $10/\lambda_3$), the steady-state charging rate is given after substitution of eq 10A and 11A by:

$$[\text{AA-tRNA}] = [A_0]tk_1k_2k_3/(k_1k_2 + k_2k_3 + k_3k_1) \quad (13A)$$

and its intercept at $t = 0$ (the burst) by:

$$I = [A_0]\frac{(k_1k_2)^2}{(k_1k_2 + k_2k_3 + k_3k_1)^2}\left[1 - \frac{k_3^2}{k_1k_2}\right] \quad (14A)$$

In order for the values of λ derived from eq 9A to be real,

$$(k_1 + k_2 + k_3)^2 \geq 4(k_1k_2 + k_2k_3 + k_3k_1) \quad (15A)$$

When this does not hold, the roots are complex numbers of the form

$$\lambda_2 = a + ib \quad (16A)$$

$$\lambda_3 = a - ib \quad (17A)$$

where,

$$a = 0.5(k_1 + k_2 + k_3) \quad (18A)$$

and

$$b = 0.5[4(k_1k_2 + k_2k_3 + k_3k_1) - (k_1 + k_2 + k_3)^2]^{1/2} \quad (19A)$$

Equations 10A and 11A still hold, but eq 6A–8A and 12A must be redrafted using de Moivre's theorem. For example,

$$[C] = [A_0]\frac{k_1k_2}{\lambda_2\lambda_3}[1 - e^{-at}(\cos bt + (a/b)\sin bt)] \quad (20A)$$

The concentration of AA-tRNA, including that bound to the enzyme, is given by:

$$[\text{AA-tRNA}] = [A_0]\frac{k_1k_2}{\lambda_2\lambda_3}\left\{1 - k_3\frac{\lambda_2+\lambda_3}{\lambda_2\lambda_3} + k_3t + e^{-at}\left(\left[\frac{k_3(\lambda_2+\lambda_3)}{\lambda_2\lambda_3} - 1\right]\cos bt - \left[\frac{k_3(a^2-b^2)}{b\lambda_2\lambda_3} + a/b\right]\sin bt\right)\right\} \quad (21A)$$

After the exponential phase has died out ($t > 10/a$), there is a linear steady-state charging rate given as before by eq 13A. This extrapolates back to the burst value given by eq 14A.

It is of interest that eq 20A and 21A represent "damped oscillations" so that in the transient phase, A, B, C and AA-tRNA are oscillating intermediates. However, the oscillations generally die out too quickly via the exponential attenuating factor to be observed.

Analysis of the Rate Constants for the Arginyl-tRNA Synthetase. The data at pH 7.2 are sufficiently good to be analyzed as follows. The linear portion of the plot of [Arg-tRNA] vs. time (Figure 3) is extrapolated back to the origin to give the burst, I. During the exponential phase of the reaction, the difference in [Arg-tRNA] between that extrapolated back to any time, t, and that experimentally observed at t is measured from the graph to give Δ[Arg-tRNA]. This has the effect of removing the terms in eq 12A and 21A that are not associated with the exponentials. Thus, when the roots of eq 9A are real:

$$\Delta[\text{Arg-tRNA}] = [A_0]\left\{\frac{(\lambda_2-k_3)(k_1-\lambda_2)}{\lambda_2k_3(\lambda_2-\lambda_3)}\left[k_1 - \lambda_3 + \frac{k_2k_3}{\lambda_2}\right]e^{-\lambda_2 t} + \frac{(\lambda_3-k_3)(k_1-\lambda_3)}{\lambda_3k_3(\lambda_3-\lambda_2)}\left[k_1 - \lambda_2 + \frac{k_2k_3}{\lambda_3}\right]e^{-\lambda_3 t}\right\} \quad (22A)$$

Similarly, when the roots are imaginary, Δ[Arg-tRNA] is equal to the exponential term in eq 21A.

It is seen from the semilog plot in Figure 4 that after the lag period Δ[Arg-tRNA] decreases according to good first-order kinetics. This shows that eq 12A holds and that the roots are real. The slope of the linear portion of the plot gives $\lambda_3 = 32.7$ s^{-1}. Using the conventional procedure for analyzing double exponentials (Fersht, 1977, page 163), λ_2 is found to be 122.2 s^{-1}.

The individual values of k_1, k_2, and k_3 are found from eq 10A, 11A, and 13A. This gives a cubic equation for the rate constants which may be solved to give the three roots, 3.16,

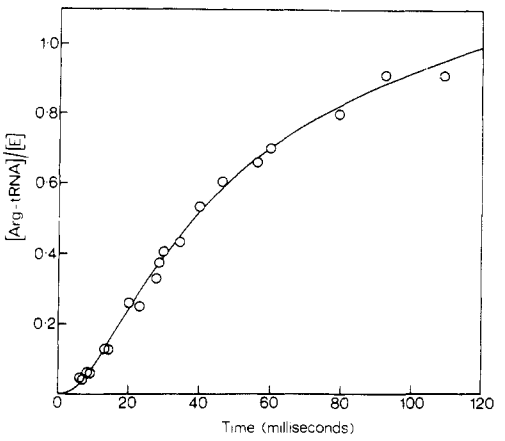

FIGURE 7: Comparison of theoretical curve and experimental data for aminoacylation at pH 7.2. The theoretical curve is calculated from substituting the derived values of k_1, k_2, and k_3 into eq 12A, allowing for only 90% saturation of the enzyme (see text).

28.5, and 123 s^{-1}. The value of 3.16 s^{-1} may clearly be assigned to k_3, since k_3 must be the smallest rate constant to give an appreciable burst (eq 14). However, as is always found in these situations, it is not possible to assign uniquely the other two values without additional experimental evidence because of the symmetry of the equations with respect to λ_2, λ_3, k_1 and k_2 (Fersht, 1977, page 113). Fortunately, the experiments on the pyrophosphate-exchange reaction (Table I) set a *lower* limit of 47 s^{-1} on k_1, which is greater than the second root of 28.5 s^{-1}. Thus, $k_1 = 123\ s^{-1}$ and $k_2 = 28.5\ s^{-1}$.

Substituting the derived values of k into eq 14A predicts a value of 0.77 for the burst, compared with the observed value of 0.68 (Table III). This small discrepancy is probably due to the enzyme's being only 90% saturated with substrates under the reaction conditions. Assuming this is so, the steady-state turnover number for charging is recalculated to be 3.1 s^{-1} (from 2.78 s^{-1}, Table III), to give: $k_1 = 123\ s^{-1}$; $k_2 = 28\ s^{-1}$; $k_3 = 3.59\ s^{-1}$.

It is seen in Figure 7 that there is excellent agreement between the theoretical curve calculated from these results and the experimental data.

The data are not sufficiently good at the other pHs to calculate the faster relaxation time and, hence, assign all three rate constants. However, since the values of the burst are similar and high below pH 7.2 and the exponential phases are rapid compared with the steady-state turnover numbers for aminoacylation, k_3 is rate determining and close in value to the steady-state turnover number. At pH 7.78, the steady-state turnover number is sufficiently high to suggest that k_3 is no longer uniquely rate determining. Accordingly, the magnitude of the burst (eq 13) drops from 0.68 at pH 7.2 to about 0.4.

The assignments of k_1, k_2, and k_3 to the three chemical steps of eq 1A are of course tentative, since there is always the possibility of slow, rate-determining, conformational changes preceding relatively rapid chemical steps.

Acknowledgments

We thank J. Weissenbach for the generous gift of $tRNA_{III}^{Arg}$. J. G. was a recipient of an EMBO Traveling Award.

References

Craine, J. E., and Peterkofsky, A. (1975), *Arch. Biochem. Biophys. 168,* 343.

Fasiolo, F., and Fersht, A. R. (1978), *Eur. J. Biochem. 85,* 85.

Fersht, A. R. (1977), Enzyme Structure and Mechanism, San Francisco, Calif., W. H. Freeman.

Fersht, A. R., and Jakes, R. (1975), *Biochemistry 14,* 3350.

Fersht, A. R., and Kaethner, M. M. (1976), *Biochemistry 15,* 818.

Fersht, A. R., Ashford, J. S., Bruton, C. J., Jakes, R., Koch, G. L. E., and Hartley, B. S. (1975), *Biochemistry 14,* 1.

Frost, A. A., and Pearson, R. G. (1961), Kinetics and Mechanism, New York, N.Y., Wiley, pp 173–176.

Gangloff, J., Schutz, A., and Dirheimer, G. (1976), *Eur. J. Biochem. 65,* 177.

Jencks, W. P. (1969), Catalysis in Chemistry and Enzymology, New York, N.Y., McGraw-Hill, p 44.

Loftfield, R. B. (1972), *Progr. Nucleic Acids Res. Mol. Biol. 12,* 87.

Mehler, A. H., and Mitra, S. K. (1967), *J. Biol. Chem. 242,* 5495.

Mulvey, R. S., and Fersht, A. R. (1977), *Biochemistry 16,* 4005.

Nazario, M., and Evans, J. A. (1974), *J. Biol. Chem. 249,* 4934.

Papas, T. S., and Peterkofsky, A. (1972), *Biochemistry 11,* 4602.

Ravel, J. M., Wang, S.-F., Heinemeyer, C., and Shive, W. (1965), *J. Biol. Chem. 240,* 432.

Yarus, M., and Berg, P. (1970), *Anal. Biochem. 35,* 450.